symmetry

MDPI

Article

Higher Order Non-Planar Electrostatic Solitary Potential in a Streaming Electron-Ion Magnetoplasma: Phase Plane Analysis

Khalid Khan [1], Manuel De la Sen [2], Muhammad Irfan [3] and Amir Ali [1,*]

[1] Department of Mathematics, University of Malakand, Chakdara 18000, Khyber Pakhtunkhwa, Pakistan
[2] Department of Electricity and Electronics, Institute of Research and Development of Processes, Faculty of Science and Technology, University of the Basque Country Campus of Leioa, 48940 Leioa, Spain
[3] Department of Physics, University of Malakand, Chakdara 18000, Khyber Pakhtunkhwa, Pakistan
* Corresponding: amiralishahs@yahoo.com

Abstract: We investigate cylindrical and spherical solitons in electron-ion (EI) plasma that contains hot (cold) electrons with stationary ions. The magneto-hydrodynamic equations are solved with the aid of the reductive perturbation (RP) technique, leading to the modified Korteweg–De Vries (mKdV) equation for the non-linear behaviour of the solitary waves in EI plasma. By employing the reduced differential transform method (RDTM), an approximate solution of the mKdV is obtained for solitary waves. Phase plane analysis reveals that these excitations exhibit periodic oscillations. The phase plane and periodic behaviour of the obtained model are studied. It is observed that the amplitude and width of the electron acoustic waves (EAWs) are affected by a slight change in the cold to hot electron temperature ratio (σ_c) and the number density of the cold to hot electron ratio (α). The effect of the streaming speed $u^{(0)}$ and superthermality index κ_e are investigated. This study is important for understanding the symmetric properties of cylindrical and spherical plasma, relying on the bifurcation analysis, impacted by the streaming effect in the EI plasma.

Keywords: plasma; electrons acoustic (EA) waves; governing equations and model; non-linear waves analysis; reduced differential transform method; phase plane analysis

Citation: Khan, K.; De la Sen, M.; Irfan, M.; Ali, A. Higher Order Non-Planar Electrostatic Solitary Potential in a Streaming Electron-Ion Magnetoplasma: Phase Plane Analysis. *Symmetry* **2023**, *15*, 436. https://doi.org/10.3390/sym15020436

Academic Editors: Abraham A. Ungar, Markus Büscher and Sergei D. Odintsov

Received: 15 December 2022
Revised: 31 January 2023
Accepted: 2 February 2023
Published: 6 February 2023

1. Introduction

The oscillation of cold electrons in an ionic field excites low-frequency electron-acoustic (EA) waves, and this is the most interesting area of research in plasma physics [1–4]. The frequency of the EA mode is much higher as compared to the ion plasma frequency, and therefore, propagations of EA waves do not impact the ions that provide a stationary background. The EA potentials have received a lot of attention due to their importance in both space and laboratory contexts. Contrary to Langmuir waves, the features of EA modes may have a spectrum that only extends approximately to the cold electron plasma frequency $(\omega_{pc} = (4\pi e^2 n_{c0}/m_e)^{\frac{1}{2}})$, where n_{c0} is the equilibrium number density of electrons, e is the electron charge, and m_e is the mass of electrons. The coherent electrostatic disturbances in space plasma are known as the EA mode [5–8]. It has also been confirmed that low-frequency excitations at electric timescales constitute linear EA waves [9,10]. Many researchers have elaborated the propagations characteristic of linear/nonlinear EA waves in diverse plasma [11]. Mace et al. [12] have reported that hot ions in an unmagnetized EI plasma involve refractive EA excitation. Similarly, it has been pointed out that the dynamics of cold electrons in super thermal plasma lead to positive polarity electrostatic perturbations [13]. Interestingly, the propagation of electrostatic as well as electromagnetic pulses is significantly altered in non-planar plasma. It has been noticed that cylindrical/spherical plasma deforms its solitary potential with the appearance of a long tail during propagation [14,15].

The most practical approach to studying nonlinear PDEs is to employ a reduction perturbation method. This method gives the linear approximation at the first order, which

is often the slowly varying envelope approximation of the considered system, described as weakly nonlinear [16–18]. On the other hand, the Lie group method is an effective method for studying conservation laws, performing Lie symmetry analysis, and finding exact solutions to nonlinear partial differential equations. In some recent findings, the symmetric analysis of spherical and cylindrical KdV has been discussed in detail [19,20]. For our purpose, we have applied a standard reductive perturbation technique and obtained the Korteweg–De Vries (KdV) equation, which admits the excitation of phase-shaped solitons. Moreover, using the reduced differential transform method (RDTM), we have obtained time-dependent solutions to the KdV equation. The numerical analysis reveals that the phase portrait of an EA soliton favours a complicated pattern of super-nonlinear waves (SNWs). It has been shown that cylindrical/spherical plasma modifies the wave profile. Moreover, the non-planar solitary excitations develop a flat tail upon propagation [21].

Here, a non-planar modified KdV is derived for electron-positron ion plasma using the reductive perturbation technique. Numerical analyses revealed that the amplitudes and width of the ion-acoustic waves decrease with increasing positron concentration. It was also found that the ion-acoustic solitary waves in cylindrical and spherical geometries in e-p-i plasma are destructively influenced by positrons and adiabatically heated ions. Further, we are interested in performing a phase plane analysis of the cylindrical and spherical KdV for superthermal plasma. Several researchers have used the classic reductive perturbation method to investigate small but finite amplitude planar waves in various plasmas in a one-dimensional case (see, for example, [22,23]). Due to the dispersive and nonlinear nature of the governing equations, the KdV or modified KdV equations for the lowest-order component in the perturbation expansion can be characterised as solitons in the long-wave limit.

The differential transform method (DTM) was proposed by Zhou in 1986 to address problems related to electrical circuits and a dynamical system considered in plasma physics [24]. The suggested method is extremely effective and strong in terms of obtaining both exact and approximative solutions to many problems in technology, finance, and engineering. The differential transform method is a Taylor series-based numerical method that produces an exact polynomial solution to a given problem. The well-known high-order Taylor series approach only necessitates symbolic computation. The reduced differential transform method (RDTM) is a more sophisticated technique [25–27]. It reduces numerical computation because it does not require any discretization, linearization, or insignificant perturbations. Further, the reduced differential transform approach has been widely used by numerous scholars [28,29]. Numerous works indicate that RDTM's solution process is much easier to understand compared to the Homotopy perturbation technique (HPM), differential transform method (DTM), the variational iteration method (VIM), and the Adomian decomposition method (ADM) [30,31]. On the other hand, computational efforts have been reduced while assuring rapid convergence and excellent precision in the numerical solution.

The paper is structured as follows: In Section 2, the fluid model equations for magnetoplasma containing cold (hot) electrons and stationary ions are presented. A reductive perturbation technique is used and a modified KdV called the cylindrical/spherical KdV equation is derived in Section 3. In Section 4, using the RDT scheme, a time-dependent solution for the mKdV equation is obtained. The conservative quantities for the modified Korteweg–De Vries (mKdV) equation are derived in Section 5. For super-nonlinear waves, a phase portrait analysis for the EA excitation is given in Section 6. The numerical results are elaborated in Section 7, while a brief summary is given in Section 8.

2. Governing Equations

We investigate electrons-ions (EI) plasma constituted of hot (cold) electrons and stationary ions. A constant magnetic field $B = B_0\hat{r}$ in the direction of propagation of the EA wave is assumed. The electrons are assumed to have a constant shear flow $u^{(0)}$, whereas the hot electrons follow the kappa distribution function. At equilibrium, $n_{s0} = n_{i0}$, where

n_s is the unaltered density of the *jth* species ($j = e$, electrons, and i ions, respectively). The nonlinear dynamics of EI waves can be governed by hydrodynamic (MHD) equations

$$\frac{\partial n_c}{\partial t} + \nabla(n_c \mathbf{u_c}) = 0, \tag{1}$$

$$m_e n_c \left(\frac{\partial \mathbf{u_c}}{\partial t} + \mathbf{u_c} \cdot \nabla \mathbf{u_c} \right) = e n_c \left(E + \frac{\mathbf{u_c}}{c} \times B \right) - \nabla P_c, \tag{2}$$

and

$$\nabla^2 \phi = 4\pi e(n_c + n_h - n_{i0}), \tag{3}$$

where the cold electron number densities, speeds, and pressures are, respectively, n_c, $\mathbf{u_c}$, and P_c. E is the electric field caused by moving charges, as calculated by $E = -\partial\phi/\partial r$. Furthermore, $\phi = \phi(r, t)$ represents the electrostatic potential, the electronic charge (mass) is represented by $e(m_e)$, and the number densities for hot electrons and ions are represented by n_h and (n_i) respectively. The distribution of hot electrons and the pressure of cold electrons are provided in the following form

$$P_c = P_{c0} \left(\frac{n_c}{n_{c0}} \right)^{\gamma}, \tag{4}$$

$$n_h = n_{h0} \left\{ 1 - \frac{e\phi}{T_h(\kappa_e - \frac{3}{2})} \right\}^{-\kappa_e + \frac{1}{2}}, \tag{5}$$

where $P_{c0} = n_{c0} T_{c0}$, n_{c0} is the number density of cold electrons at equilibrium with temperature T_{c0}, γ is the adiabatic constant, the special index (κ_e) accounts for the superthermal hot electrons, and T_h is the temperature of the hot electrons.

In polar form, Equations (1)–(3) can be written as

$$\frac{\partial \bar{n}_c}{\partial t} + u^{(0)} \left(\frac{v}{r} \bar{n}_c + \frac{\partial}{\partial r} \bar{n}_c \right) + \frac{v}{r} \bar{n}_c \bar{\mathbf{u}}_\mathbf{c} + \frac{\partial}{\partial r} \bar{n}_c \bar{\mathbf{u}}_c = 0, \tag{6}$$

$$\frac{\partial \bar{\mathbf{u}}_\mathbf{c}}{\partial t} + \mathbf{u}^{(\mathbf{0})} \frac{\partial \bar{\mathbf{u}}_\mathbf{c}}{\partial r} + \bar{\mathbf{u}}_\mathbf{c} \frac{\partial \bar{\mathbf{u}}_\mathbf{c}}{\partial r} = -\frac{\partial \bar{\phi}}{\partial r} - \frac{\sigma_c}{(1-\alpha)^{\gamma-1}} \gamma (\bar{n}_c)^{\gamma-1} \frac{\partial \bar{n}_c}{\partial r}, \tag{7}$$

and

$$\frac{\partial^2 \bar{\phi}}{\partial r^2} + \frac{v}{r} \frac{\partial \bar{\phi}}{\partial r} = \bar{n}_c + \alpha n_h - 1, \tag{8}$$

where $\bar{n}_c = n_c/n_{c_0}$ represents the normalised number densities of cold electrons, $\bar{u_c} = (\mathbf{u_c} = \mathbf{u}^{(\mathbf{0})} + \mathbf{u_c})/c_s$ represents its normalised velocity, $\bar{\phi} = e\phi/T_h$ represents the normalised electrostatic potential of EA waves, and $c_s = \sqrt{T_h/m_e}$ represents EA speed. $\omega_{pc} = \sqrt{4\pi e^2 n_{c0}/m_e}$ normalizes the time (t), whereas r is normalized by the Debye length $\lambda_D = \sqrt{T_h/4\pi e^2 n_{c0}}$. $\sigma_c = T_h/T_c$ is the cold to hot temperatures ratio, and $\alpha = n_{h0}/n_{c0}$ is the ratio of the number densities of cold to hot electrons. Using binomial expansion, Equation (5) takes the form

$$n_h = n_{h0} \left(1 + c_1 \bar{\phi} + c_2 \bar{\phi}^2 + \cdots\cdots \right), \tag{9}$$

where

$$c_1 = -(-\kappa_e + \frac{1}{2})/(\kappa_e - \frac{3}{2}), \quad c_2 = (-\kappa_e + \frac{1}{2})(-\kappa_e - \frac{1}{2})/(\kappa_e - \frac{3}{2})^2.$$

3. Non-Linear Wave Analysis

For simplicity, we remove the bars on the variables in Equations (6)–(8) and apply the RPM technique to obtain a cylindrical and spherical KdV model for the EI plasma by expanding the variables in Equations (6)–(8) to examine the nonlinear propagation of the EA waves in the following manner

$$\begin{pmatrix} n_c \\ u_c \\ \phi \end{pmatrix} = \begin{pmatrix} 1 \\ 0 \\ 0 \end{pmatrix} + \epsilon \begin{pmatrix} n_c^{(1)} \\ u_c^{(1)} \\ \phi^{(1)} \end{pmatrix} + \epsilon^2 \begin{pmatrix} n_c^{(2)} \\ u_c^{(2)} \\ \phi^{(2)}, \end{pmatrix} + \cdots . \tag{10}$$

We further introduce the stretched variables to find a nonlinear solution of small amplitude acoustic solitary waves in EI plasma

$$\xi = -\epsilon^{\frac{1}{2}}(x + \lambda t), \quad \tau = \epsilon^{\frac{3}{2}} t, \tag{11}$$

where ϵ is a small parameter indicating nonlinearity and dispersion weakness and λ is the phase velocity of EA waves normalised by c_s. The differential relations can therefore be written as follows

$$\frac{\partial}{\partial x} \to -\epsilon^{\frac{1}{2}} \frac{\partial}{\partial \xi}, \quad \frac{\partial}{\partial t} \to \left(-\epsilon^{\frac{1}{2}} \lambda \frac{\partial}{\partial \xi} + \epsilon^{\frac{3}{2}} \frac{\partial}{\partial \tau} \right). \tag{12}$$

Putting Equations (10)–(12) in Equations (6)–(8), we obtain lower orders of ϵ hierarchy-equations in the form

$$n_c^{(1)} = \alpha c_1 \phi^{(1)}, \quad u_c^{(1)} = -\frac{\phi^{(1)}}{(u^{(0)} + \lambda)}, \quad \lambda = -u^{(0)} \pm \sqrt{1 + u^{(}(0))^2 (1 - \alpha c_1)}. \tag{13}$$

Similarly,

$$\begin{aligned} &\frac{\partial}{\partial \xi} u_c^{(2)} + (u^{(0)} + \lambda) \frac{\partial}{\partial \xi} n_c^{(2)} + \frac{\partial}{\partial \tau} n_c^{(1)} + \frac{v}{\lambda \tau} u_c^{(1)} + \frac{\partial}{\partial \xi} n_c^{(1)} u_c^{(1)} = 0, \\ &(u^{(0)} + \lambda) \frac{\partial}{\partial \xi} u_c^{(2)} - \frac{\partial}{\partial \tau} u_c^{(1)} + u_c^{(1)} \frac{\partial}{\partial \xi} u_c^{(1)} + \frac{\partial}{\partial \xi} \phi_2 + \frac{\sigma_c \gamma (\gamma - 1)}{(u^{(0)} + \lambda)(1 - \alpha)} n_c^{(1)} \frac{\partial}{\partial \xi} n_c^{(1)} = 0, \\ &\frac{\partial^2}{\partial \xi^2} \phi^{(1)} - n_c^{(2)} + \alpha c_1 \phi^{(2)} + \frac{\alpha c_2}{2} (\phi^{(1)})^2 = 0. \end{aligned} \tag{14}$$

Combining Equations (13) and (14), we obtain the mKdV equation in the form

$$\frac{\partial}{\partial \tau} \phi^{(1)} + \frac{v}{2\tau} \phi^{(1)} + A \phi^{(1)} \frac{\partial}{\partial \xi} \phi^{(1)} + B \frac{\partial^3}{\partial \xi^3} \phi^{(1)} = 0, \tag{15}$$

where $A = A_2 / A_1$ and $B = 1/A_1$ with $a_0 = \frac{\sigma_c}{(1-\alpha)^{\gamma-1}}$ and

$$\begin{aligned} A_1 &= \frac{\alpha c_1 \left(a_0 \gamma + (\lambda + (u^{(0)})^2 \right) + 2}{(\lambda + u^{(0)}) \left((\lambda + (u^{(0)})^2) - a_0 \gamma \right)}, \\ A_2 &= \frac{\alpha^2 a_0 \gamma c_1^2 \left(-a_0 \gamma + \lambda(\gamma + 2\lambda - 1) + 2(u^{(0)})^2 + u^{(0)}(\gamma + 4\lambda - 1) \right)}{(\lambda + (u^{(0)})^2) \left(((\lambda + (u^{(0)})^2) - a_0 \gamma \right)} \\ &+ \frac{4 \alpha c_1 \left((\lambda + (u^{(0)})^2) - a_0 \gamma \right) - 4}{(\lambda + (u^{(0)})^2) \left(((\lambda + (u^{(0)})^2) - a_0 \gamma \right)} - \alpha c_2. \end{aligned} \tag{16}$$

4. Applications of RDTM

To apply RDTM to our derived model (15), we can write

$$D_\tau \phi + A\phi D_\xi \phi + BD_{\xi\xi\xi}\phi + \frac{v}{2}\tau^{-1}\phi = 0, \tag{17}$$

where $\phi = \phi^{(1)}(\xi, \tau)$. The exact solution for system (17) is given by [32]

$$\phi(\xi, \tau) = \frac{\xi}{2A\tau} + \frac{12B^{1/3}}{A\tau}\sec h^2\left(\frac{\xi + 8B^{1/3}}{B^{1/3}\sqrt{\tau}}\right). \tag{18}$$

We start with one-dimensional planar geometry ($v = 0$) and investigate the stationary solitary wave solution of Equation (15). Consider the initial condition

$$\phi(\xi, 0) = \phi_m \text{sech}^2\left(\frac{\xi}{\Delta}\right), \tag{19}$$

where A, and B are given in Equation (15) and $D_\tau = \partial/\partial\tau$, $\quad D_\xi = \partial/\partial\xi$ with $\phi_m = \frac{3\lambda}{A}$ and $\Delta = \sqrt{\frac{4B}{\lambda}}$. Next, applying RDTM given in Appendix A to Equation (17), we get

$$\Phi_{j+1}(\xi) = \frac{1}{j+1}\left[-A\sum_{r=0}^{j}\Phi_j(\xi)D_\xi\Phi_{j-r}(\xi) - BD_{\xi\xi\xi}\Phi_j(\xi) - \frac{v}{2}\delta(j+1)\Phi_j(\xi)\right], \tag{20}$$

from the initial condition (19), we have

$$\Phi_0(\xi) = \phi_m \text{ sech}^2\left(\frac{\xi}{\Delta}\right). \tag{21}$$

Putting $j = 0, 1, 2$ in Equation (20), we obtain

$$\begin{aligned}
\Phi_1(\xi) &= -A\Phi_0(\xi)D_\xi\Phi_0(\xi) - BD_{\xi\xi\xi}\Phi_0(\xi) - \frac{v}{2}\delta(1)\Phi_0(\xi),\\
\Phi_2(\xi) &= -\frac{1}{2}\left[A\left(\Phi_0(\xi)D_\xi\Phi_1(\xi) + \Phi_1(\xi)D_\xi\Phi_0(\xi)\right) + BD_{\xi\xi\xi}\Phi_1(\xi) + \frac{v}{2}\delta(2)\Phi_1(\xi)\right],\\
\Phi_3(\xi) &= -\frac{1}{3}\Big[A\left(\Phi_0(\xi)D_\xi\Phi_2(\xi) + \Phi_1(\xi)D_\xi\Phi_1(\xi) + \Phi_2(\xi)D_\xi\Phi_0(\xi)\right)\\
&+ BD_{\xi\xi\xi}\Phi_2(\xi) + \frac{v}{2}\delta(3)\Phi_2(\xi)\Big].
\end{aligned} \tag{22}$$

Applying the inverse differential transform (A7) to Equation (21) and Theorem A2, we obtain

$$\begin{aligned}
\phi_0 &= \phi_m \text{sech}^2\left(\frac{\xi}{\Delta}\right),\\
\phi_1 &= \frac{\tau}{\Delta^3}2\phi_m \tanh\left(\frac{\xi}{\Delta}\right)\text{sech}^4\left(\frac{\xi}{\Delta}\right)\left(A\Delta^2\phi_m + 2B\left(\cosh\left(\frac{2\xi}{\Delta}\right) - 5\right)\right),\\
\phi_2 &= \frac{\tau^2\phi_m}{8\Delta^4}\Big[8A^2\Delta^2\phi_m^2\left(3\cosh\left(\frac{2\xi}{\Delta}\right) - 4\right) + 2A\phi_m\Big(-\left(152B + \Delta^2 v\right)\cosh\left(\frac{2\xi}{\Delta}\right)\\
&+ \left(8B + \Delta^2 v\right)\cosh\left(\frac{4\xi}{\Delta}\right) + 176B - 2\Delta^2 v\Big) + 4B\cosh^2\left(\frac{\xi}{\Delta}\right)\Big(-26v\cosh\left(\frac{2\xi}{\Delta}\right)\\
&+ v\cosh\left(\frac{4\xi}{\Delta}\right) + 33v - 10\Delta\sinh\left(\frac{2\xi}{\Delta}\right) + \Delta\sinh\left(\frac{4\xi}{\Delta}\right)\Big)\Big]\text{sech}^8(\xi).
\end{aligned} \tag{23}$$

Other terms can be calculated in a similar way. Finally, up to the 4th order, we can write

$$\phi(\tau,\xi)=\sum_{j=0}^{2}\left[\frac{1}{j!}\phi_j\left(\frac{\xi}{\Delta}\right)\right]t^j. \tag{24}$$

One can see that, for larger values of $j\to\infty$, the approximate solution (24) approaches the exact solution (18).

5. Conservation Laws for the Model (15)

The existence of an infinite number of conservation laws is one of the most intriguing features of KdV systems. Let us start with the derivation of a few fundamental conservation laws. An elegant generalisation of Miura's transformation yields a compelling argument for the existence of an infinite number of conservation laws. Consider the following Miura transformation [33]

$$\phi^{(1)}=\psi-\epsilon\partial_{\xi}\psi-\epsilon^2\psi^2. \tag{25}$$

Putting Equation (25) in Equation (15), we obtain

$$\begin{aligned}&\frac{\partial}{\partial\tau}\left(\psi-\epsilon\partial_{\xi}\psi-\epsilon^2\psi^2\right)+\frac{v}{2\tau}\left(\psi-\epsilon\partial_{\xi}\psi-\epsilon^2\psi^2\right)\\&+A\left(\psi-\epsilon\partial_{\xi}\psi-\epsilon^2\psi^2\right)\frac{\partial}{\partial\xi}\left(\psi-\epsilon\partial_{\xi}\psi-\epsilon^2\psi^2\right)+B\frac{\partial^3}{\partial\xi^3}\left(\psi-\epsilon\partial_{\xi}\psi-\epsilon^2\psi^2\right)=0.\end{aligned} \tag{26}$$

Consider the series solution of the transform Equation (26)

$$\psi(\xi,\tau,\epsilon)=\sum_{n=0}^{\infty}\epsilon^n\psi_n(\xi,\tau), \tag{27}$$

then the Miura transformation (25) takes the following form

$$\phi^{(1)}=\sum_{n=0}^{\infty}\epsilon^n\psi_n(\xi,\tau)-\epsilon\partial_{\xi}\left(\sum_{n=0}^{\infty}\epsilon^n\psi_n(\xi,\tau)\right)-\epsilon^2\left(\sum_{n=0}^{\infty}\epsilon^n\psi_n(\xi,\tau)\right)^2, \tag{28}$$

Equating ϵ powers, we obtain the following conserved quantities

$$\begin{aligned}&\phi^{(1)}=\psi_0,\\&\psi_1-\partial_{\xi}\psi_0=0,\\&\psi_2-\partial_{\xi}\psi_1-\psi_0^2=0,\\&\psi_3-\partial_{\xi}\psi_2-2\psi_0\psi_1=0,\\&\vdots\end{aligned} \tag{29}$$

Solving these equations recursively, we get

$$\begin{aligned}&\phi^{(1)}=\psi_0,\\&\psi_1=\partial_{\xi}\phi^{(1)},\\&\psi_2=2(\phi^{(1)})^3-(\partial_{\xi}\phi^{(1)})^2,\\&\psi_3=\partial_{\xi}^3\phi^{(1)}+4\phi^{(1)}\partial_{\xi}\phi^{(1)},\\&\vdots\end{aligned} \tag{30}$$

From these, one can derive the following conservative quantities, that is, mass (M), momentum (P) and energy (E). These quantities are represented by the following equations

$$M = \int_{-\infty}^{+\infty} \phi^{(1)} d\xi = \text{constant}, \quad P = \int_{-\infty}^{+\infty} (|\phi^{(1)}|^2 d\xi = \text{constant},$$
$$E = \int_{-\infty}^{+\infty} 2(\phi^{(1)})^3 - (\partial_\xi \phi^{(1)})^2 d\xi = \text{constant}.$$

The following Table 1 shows the conservative quantities for different values of τ and ξ.

Table 1. Evaluation of the conservative quantities against the temporal variable τ and spacial variable ξ.

τ	ξ	M	P	E	$\phi(\xi, \tau)$
0.1	1.0	3.99999	1.59999	4.45358	0.57027
0.2	2.0	3.99999	1.59999	4.45358	0.45624
0.2	4.0	3.99999	1.59999	4.45358	0.39767
0.6	6.0	3.99999	1.59999	4.45358	0.26558
0.8	8.0	3.99999	1.59999	4.45358	0.11984
1.0	10.0	3.99999	1.59999	4.45358	0.09583

6. Phase Plane Analysis

A phase portrait is a graphical tool that shows how the solutions of a differential equation will behave over time. For plasma systems with more than three separate components, phase portrait profiles are more complicated, resulting in more fascinating wave patterns. The number of fixed points and separatrices in phase plots evolves with wave-matching trajectories. The bifurcation in dynamical systems [34] is a major change in the system as a result of a change in a physical parameter. The underlying properties of dynamical systems are revealed through phase plane analysis utilising bifurcation theory. Any qualitative circle in the phase plane is said to correspond to a travelling wave solution [35]. In light of bifurcation analysis, the qualitative phase pictures for dynamical systems (15) are presented. For phase plane analysis, consider $\phi(\xi, \tau) = \phi(\zeta)$ with $\zeta = (\xi - \lambda\tau)$; then Equation (15) can be written as

$$-\lambda \frac{d}{d\zeta}\phi(\zeta) + \frac{v}{2\tau}\phi(\zeta) + A\frac{\phi(\zeta)}{d\zeta}\phi(\zeta) + B\frac{d^3}{d\zeta^3}\phi(\zeta) = 0. \tag{31}$$

Integrating Equation (31) with respect to ζ and considering for $\zeta \to \pm\infty$, $d\phi/d\zeta \to 0$ and $d^2\phi/d\zeta^2 \to 0$, we obtain the following system of ordinary differential equation

$$\begin{cases} \frac{d\phi}{d\zeta} = z = f(\phi, z), \\ \frac{dz}{d\zeta} = \frac{1}{B}\left(\lambda\phi - \frac{A}{2}\phi^2\right) + \frac{v}{2\tau}\int_0^\zeta \phi(\zeta)d\zeta = g(\phi, z). \end{cases} \tag{32}$$

The Jacobian matrix for the system (32) is defined by

$$J = \begin{pmatrix} \frac{\partial f(\phi,z)}{\partial \phi} & \frac{\partial f(\phi,z)}{\partial \zeta} \\ \frac{\partial g(\phi,z)}{\partial \phi} & \frac{\partial g(\phi,z)}{\partial \phi} \end{pmatrix} = \begin{pmatrix} 0 & 1 \\ \frac{1}{B}(\lambda - A\phi_i) & 0 \end{pmatrix}. \tag{33}$$

The determinant of the Jacobian is determined by

$$\mathfrak{D} = detJ(\phi_i, 0) = -\frac{1}{B}(\lambda - A\phi_i), \tag{34}$$

To obtain the fixed points of the system (32), considering $d\phi/d\zeta = 0$ and $dz/d\zeta = 0$, we obtain the fixed points $P_0(\phi_0, 0), P_1(\phi_1, 0)$ where

$$\phi_0 = 0, \quad \phi_1 = \frac{2\lambda}{A}.$$

For phase plane analysis of the system (32), the determinant (34) is very much important in the sense of $i = 0, 1$ if $\mathfrak{D} < 0$; then the point $P_i(\phi_i, 0)$ is the saddle point and for $\mathfrak{D} > 0$, the point $P_i(\phi_i, 0)$ is the centre point of the system (32) (see [34]).

7. Results and Discussion

For numerical illustrations, we have chosen some typical parameters of a magnetoplasma, with cold (superthermal) electrons and stationary ions being relevant to the ionosphere as well as to laboratory scenarios. The number density and magnetic field ranges are $n_{c0} = 10^{18}$–10^{19}cm^{-3} and $B_0 = 10^5$–10^6 G, respectively. The most important results are highlighted and Figure 1a illustrates the phase speed (λ) of a non-planar EA wave as a function of the superthermality index (κ_e) with variations in the streaming speed ($u^{(0)}$). Notice that the index κ_e raises the concentration of high energy electrons and in turn enhances the wave phase speed. Similarly, the streaming speed modifies the electron dynamics and results in the propagation of EA pulses at a relatively high speed. We have depicted in Figure 1b the phase speed (λ) versus the superthermal index (κ_e) at different values of the cold to hot electron temperature ratio (σ_c). This reveals that thermal correction due to random motion increases λ. The solution (24) for EA soliton is given in Figure 2a against spatial variable (ξ) when the variable $\gamma = 1$ (solid curve), 2 (dashed curve), or 3 (dotted curve). Obviously, the variations reduce the amplitude of the wave profile by increasing the values of the parameter from 1 to 3. The profile of EA pulses in Figure 2b at different values of κ_e reveals that energetic electrons raise the amplitude as well as the width of the EA potential. Similarly, the wave solution depicted with variations in, for Figure 2c, temperature ratios and, for Figure 2d, streaming speed, admits significant modification.

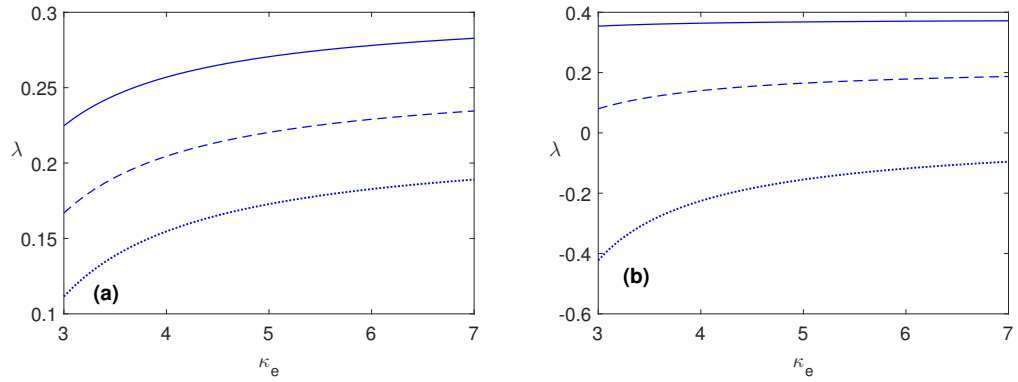

Figure 1. The phase speed (λ) given in Equation (24) against κ_e by changing (**a**) $u^{(0)}$ = 1 (solid line), 1.1 (dashed line), 1.2 (dotted line) and (**b**) α = 0.1 (solid line), 0.5 (dashed line), 1 (dotted line).

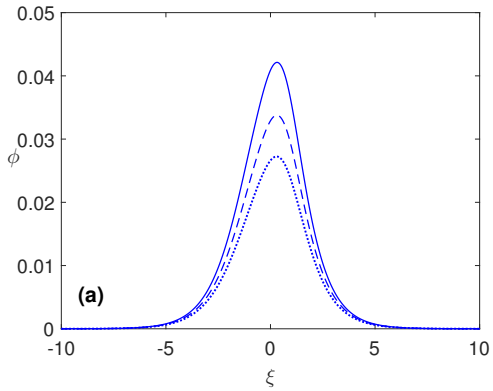

Figure 2. *Cont.*

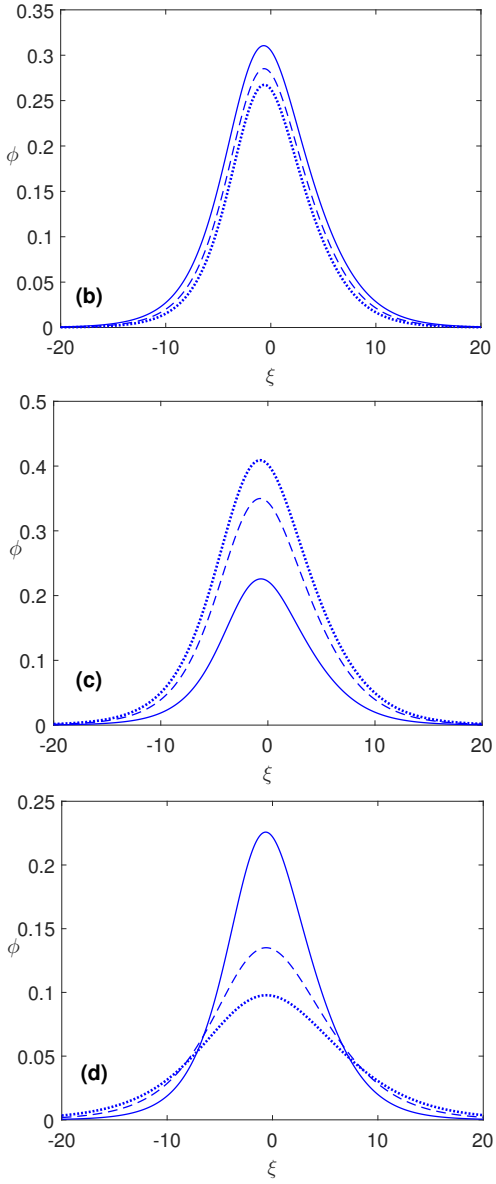

Figure 2. The profiles of solitary waves for $\sigma_c = 0.3, \lambda = 0.2$ based on Equation (24) plotting the electrostatic potential Φ against the spatial coordinate ξ by changing (**a**) $\gamma = 1$ (Solid curve), $\gamma = 2$ (dashed curve), $\gamma = 3$ (dotted curve), (**b**) changing refractive index $\kappa_e = 3$ (solid curve), $\kappa_e = 5$ (dashed curve), $\kappa_e = 7$ (dotted curve), (**c**) changing the cold to hot electrons temperature ratio $\alpha = 0.4$ (solid curve), $\alpha = 0.5$ (dashed curve), $\alpha = 0.6$ (dotted curve) and (**d**) changing the plasma streaming effect $u^{(0)} = 0.3$ (solid curve), $u^{(0)} = 0.5$ (dashed curve), $u^{(0)} = 0.7$ (dotted curve).

For larger time span, the waves start oscillation between -1 and 1 for both cylindrical and spherical cases as we have shown in Figure 3a and Figure 3b, respectively. The temporal variable τ in the model modifies the amplitude and width of the wave profile. In Figure 4a, we traced the direction field of the system (32) for cylindrical ($v = 1$) and spherical ($v = 2$) for different parameters ($\sigma_c = 0.2$, $\lambda = 0.1$). Similarly, a phase portrait of the system (32) with $\sigma_c = 0.5$, $\lambda = 0.3$ and $\alpha = 0.2$ is given in Figure 5 for (a) cylindrical KdV ($v = 1$) and (b) for spherical KdV ($v = 2$). It can be observed that, in both cases, there is the saddle point $P_0(0, 0)$ and the centre at $P_1(\phi_1, 0)$. A phase portrait of the system (32) with $\sigma_c = 0.5$, $\lambda = 0.3$ in for cylindrical KdV ($v = 1$) (a) $\alpha = 0.09$ and (b) $\alpha = 0.1$ for spherical KdV ($v = 2$) is shown Figure 6. It can be observed that a nonlinear homoclinic orbit (NHO) about $P_0(0, 0)$ enclosing fixed point $P_1(\phi_1, 0)$ and nonlinear periodic orbit (NPO) enclosing the fixed point $P_1(\phi_1, 0)$ correspond to EA waves. However, when we take the parameters values to unity,

we get periodic waves of the system about $P_0(0,0)$, as shown in Figure 7a,b. The effect of the parameter κ_e on the periodic waves for large values of time parameter $\tau = 20$ is shown in Figure 8a,b for both cylindrical and spherical KdV. The conserved quantities momentum, mass and energy derived four our model in Section 5 are numerically shown in Table 1. We see that all these conserved quantities are unaffected with the passage of time.

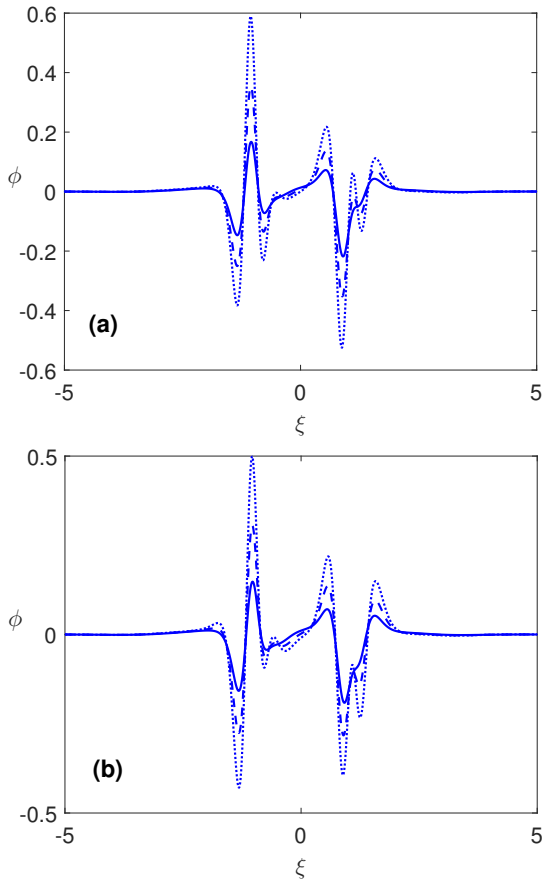

Figure 3. The oscillatory wave profiles for Equation (24) for different values of the parameters as given in Figure 2 for larger temporal variable as (**a**) $\tau = 1$ (solid curve), $\tau = 2$ (dashed curve) and $\tau = 3$ (dotted curve) curves in cylindrical KdV (v = 1) and (**b**) $\tau = 1$ (solid curve), $\tau = 2$ (dashed curve) and $\tau = 3$ (dotted curve) curves in spherical KdV (v = 2).

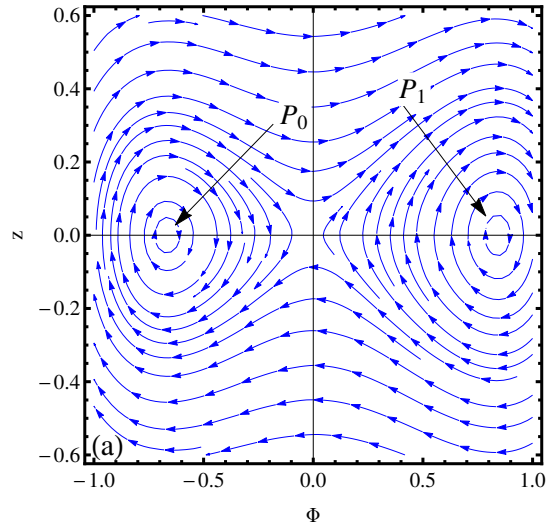

Figure 4. *Cont.*

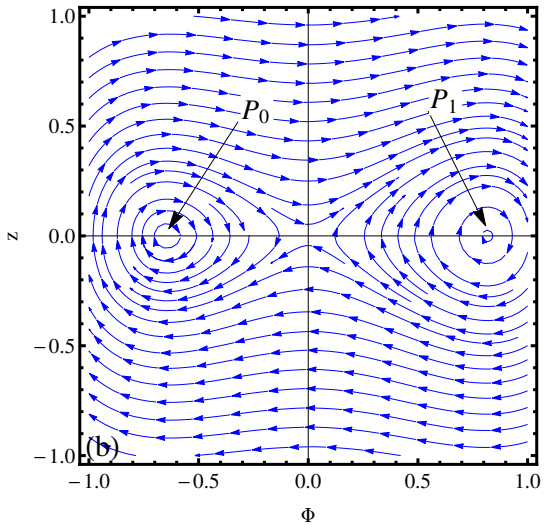

Figure 4. Direction field lines of EI plasma referring to system (32) with $\sigma_c = 0.2$, $\lambda = 0.1$, $\kappa_e = 3$ and $\alpha = 0.01$ for (**a**) cylindrical ($v = 1$) and (**b**) spherical ($v = 2$).

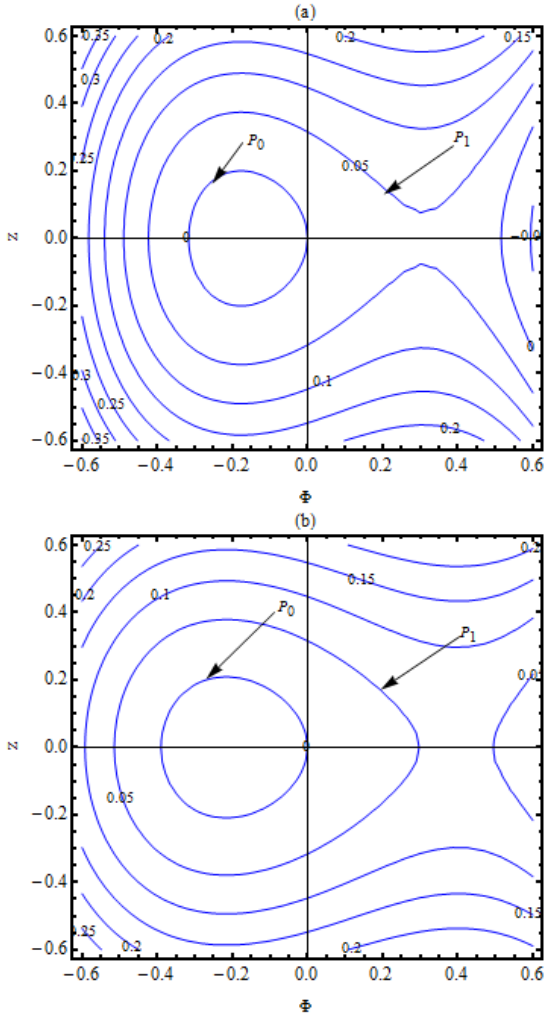

Figure 5. Phase portrait of EI plasma referring to system (32) with $\sigma_c = 0.5$, $u^{(0)} = 1$, $\lambda = 0.3$, $\alpha = 0.2$ and $\kappa_e = 1.6$ for (**a**) cylindrical ($v = 1$) and (**b**) spherical ($v = 2$).

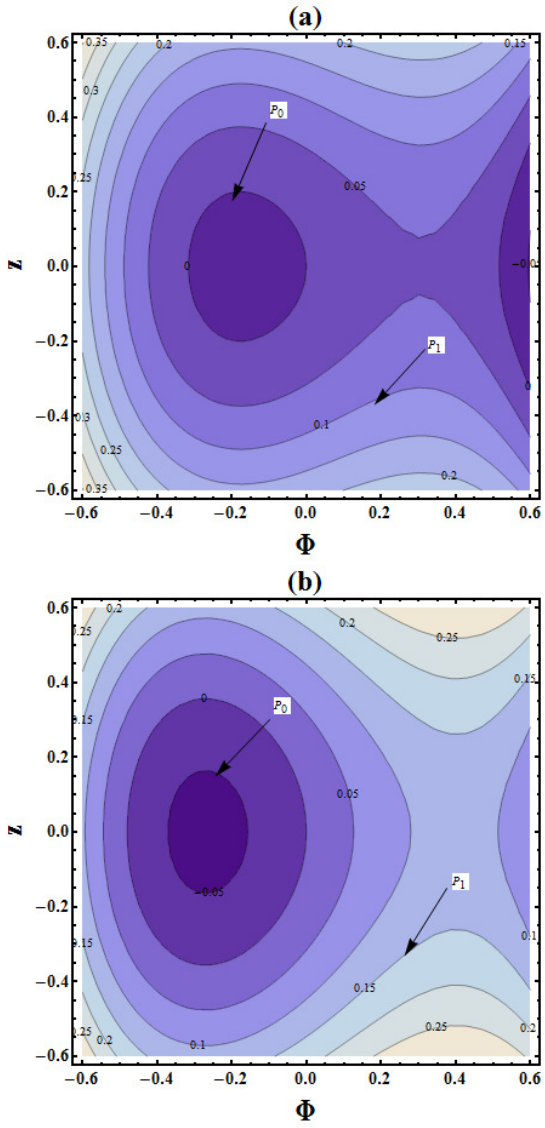

Figure 6. Contours for EI plasma referring to system (32) with $\sigma_c = 0.5$, $u^{(0)} = 1$, $\lambda = 0.3$, $\alpha = 0.2$ and $\kappa_e = 1.65$ for (**a**) cylindrical ($v = 1$) and (**b**) spherical ($v = 2$).

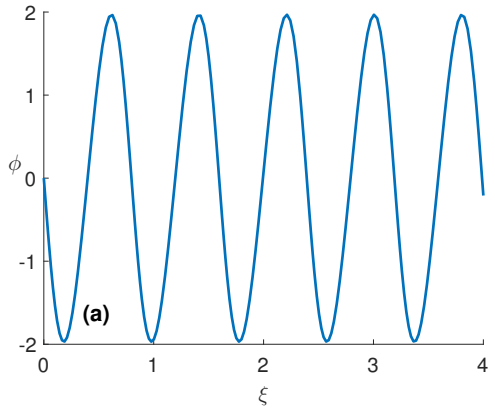

Figure 7. *Cont.*

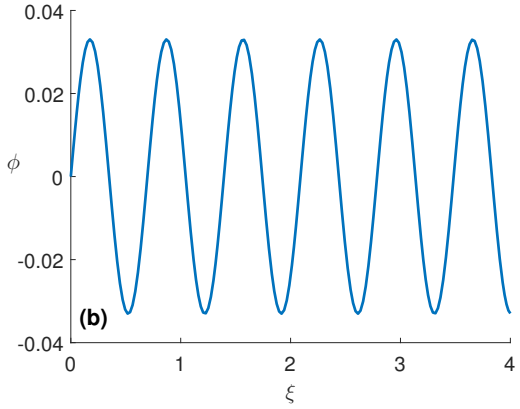

Figure 7. The oscillatory profile of the system (32) with $\sigma_c = 1$, $\lambda = 1$, $\gamma = 1$, $\alpha = 1$ and (**a**) $\kappa_e = 5$ for cylindrical ($v = 1$) KdV (**b**) $\kappa_e = 7$ for spherical KdV ($v = 2$).

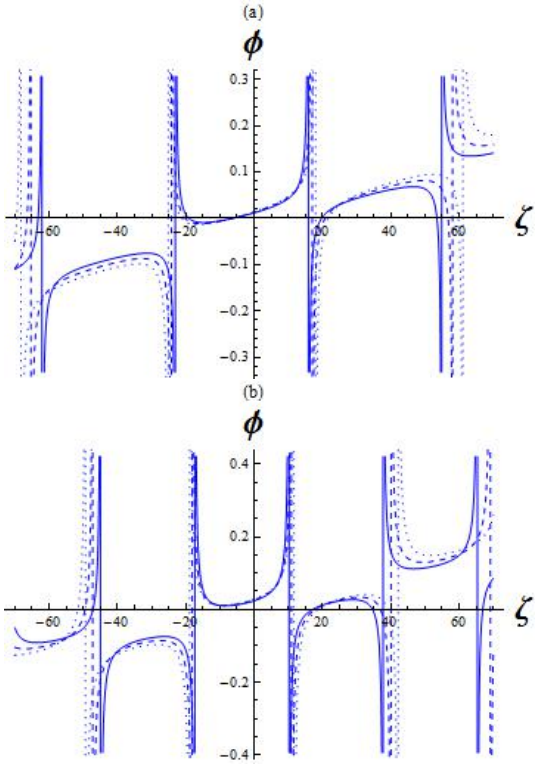

Figure 8. Periodic waves of the system (32) for larger time ($\tau = 20$) with $\sigma_c = 1$, $\lambda = 0.52$, $\gamma = 0.43$, $\alpha = 1$ and (**a**) for cylindrical ($v = 1$) KdV (**b**) for spherical KdV ($v = 2$) with $\kappa_e = 1.6$ (solid), 1.62 (dashed) and 1.64 (dotted).

8. Conclusions

Cylindrical and spherical KdV models for EI plasma with hot and cold electrons and stationary ions were derived using the reductive perturbative (RP) method. For the first time, the cold electrons following the constant shear flow $u^{(0)}$ in the KdV model are considered. An analytical method called the reduced differential transform method is applied to calculate an approximate solution to the model. It is observed that for smaller values of the temporal variable τ the approximate solution (24) converges to the exact solution (18) of the model. It is shown that, when the temperature of hot electrons is low, a small-amplitude EAW develops. When a small-amplitude EAW grows smoother, the spectral index of electrons approaches the Maxwellian limit. As a result, our findings indicate the presence of small-amplitude nonlinear electron acoustic waves (EAWs) in plasmas with distributed cold and hot electrons. Studying the non-planar convergence in

such plasmas, in the presence of cold and hot electrons with stationary ions, specifically electrons and ions, is significant because the non-planar wave is crucial to understanding inertial confinement fusion as well as space laboratory plasmas. Since we are interested in seeing how the ratio α, the super thermal index κ_e and the streaming speed $u^{(0)}$ of the cold electrons affect the non-planar wave profile, we took the temperature ratio of cold to hot electrons as being smaller than unity to see how this ratio affects the wave profile. The geometry has a major influence on the non-planar wave. As the distance from the spherical or cylindrical geometry's centre grows, the non-planar waves progressively weaken. The pressure density behind the wave front changes as it moves forward and backward, which is how this occurs physically.

The qualitative phase portrait profiles for dynamical systems (32) were illustrated using the bifurcation theory of dynamical systems. The NPO and NHO of the dynamical system generated from the KdV Equation (15) support the EAW solutions. The presence of a small amplitude EAW solution of the KdV equation in the investigated plasma system was discovered for the first time using bifurcation through phase plane analysis.

Author Contributions: Conceptualization: K.K., M.D.l.S., M.I., A.A.; Methodology: K.K., M.D.l.S., M.I., A.A.; Software: K.K., M.I., A.A.; Validation: K.K., M.I., A.A.; Formal analysis: K.K., M.D.l.S., M.I., A.A.; Investigation: K.K., M.D.l.S., M.I., A.A.; Resources: K.K., A.A.; Data curation: K.K., M.D.l.S., M.I., A.A.; Writing—original draft preparation: K.K., M.I., A.A.; Writing—review and editing: K.K., M.D.l.S., M.I., A.A.; Visualization: K.K., M.I., A.A.; Supervision: A.A.; Project administration: M.D.l.S., A.A.; funding acquisition: M.D.l.S. All authors have read and agreed to the published version of the manuscript.

Funding: Basque Government: Grant IT1555-22 Basque Government: Grant KK-2022/00090 MCIN/AEI 269.10.13039/501100011033: Grant PID2021-1235430B-C21/C22.

Data Availability Statement: The data regarding this manuscript are available within the manuscript.

Conflicts of Interest: It is declared that all authors have no conflict of interest regarding this manuscript.

Appendix A

Appendix A.1. One-Dimensional RDTM

The jth derivative of a function $\phi(t)$ in one variable is transformed as follows: If $\phi(t) \in R$ can be written as a Taylor series around the fixed point t_0, then $\phi(t)$ can be written as

$$\phi(t) = \sum_{j=0}^{\infty} \frac{\phi^{(j)}(t_0)}{j!}(t-t_0)^j. \tag{A1}$$

Similarly, if $\phi_n(t) = \sum_{j=0}^{n} \frac{\phi^{(j)}(t_0)}{j!}(t-t_0)^j$ is the nth partial sum of the expansion (A1), then we have

$$\phi(t) = \sum_{j=0}^{n} \frac{\phi^{(j)}(t_0)}{j!}(t-t_0)^j + R_n(t), \tag{A2}$$

where $R_n(t)$ is the remainder term and nth is the Taylor polynomial for $\phi(t)$ around t_0. The differential transform $\Phi(j)$ of the function $\phi(t)$ is defined by

$$\Phi(j) = \frac{1}{j!}\left[\frac{d^j\phi(t)}{dt^j}\right]_{t=t_0}, \quad j = 0, 1, 2, \cdots \infty, \tag{A3}$$

and Equation (A1) reduced to

$$\phi(t) = \sum_{j=0}^{n} \Phi(j)(t-t_0)^j, \tag{A4}$$

and the nth partial sum of Equation (A2) takes the form

$$\phi_n(t) = \sum_{j=0}^{n} \Phi(j)(t-t_0)^j + R_n(t). \tag{A5}$$

Appendix A.2. Two-Dimensional Reduced Differential Transform Method

Consider the function $\phi(x,t)$, such that $\phi(x,t) = f(x)g(t)$. It can be represented as follows based on the properties of one-dimensional DTM:

$$\phi(x,t) = \sum_{i=0}^{\infty} P(i)(x)^i \sum_{i=0}^{\infty} Q(j)(t)^j = \sum_{i=0}^{\infty}\sum_{j=0}^{\infty} R(i,j)x^i t^j, \tag{A6}$$

where $R(i,j) = P(i)Q(j)$ is called the spectrum of the two-dimensional function $\phi(x,t)$. If $\phi(x,t)$ is the analytic function in some specific domain of interest then the spectrum function

$$\Phi_j(x,t) = \frac{1}{j!}\left[\frac{\partial^j}{\partial t^j}\phi(x,t)\right]_{t=t_0}, \tag{A7}$$

is the reduced transform function of $\phi(x,t)$ and its inverse reduce transform is defined by

$$\phi(x,t) = \sum_{j=0}^{\infty} \Phi_j(x)(t-t_0)^j, \tag{A8}$$

Combining Equations (A7) and (A8), we obtain

$$\phi(x,t) = \sum_{j=0}^{n} \frac{1}{j!}\left[\frac{\partial^j}{\partial t^j}\phi(x,t)\right]_{t=t_0}. \tag{A9}$$

Equation (A9) is the Taylor series expansion of $\phi(x,t)$ around $t = t_0$.

Appendix A.3. Analysis on RDTM

Here, we consider the following non-linear partial differential equation

$$L\phi(x,t) + R\phi(x,t) + N\phi(x,t) = 0, \tag{A10}$$

with the following initial condition

$$\phi(x, t=0) = \phi_0,$$

where L and R are the linear operators and N is a non-linear operator, then applying the RDTM to Equation (A10) with Theorems A1–A3, we obtain the following recursive relation

$$(j+1)\Phi_{j+1}(x) + R\Phi_j(x) + N\Phi_j(x) = 0. \tag{A11}$$

Theorem A1. *If* $\phi(x,t) = \frac{\partial^n}{\partial t^n}\phi(x,t)$, *then* $\Phi_j(x) = \frac{(j+n)!}{j!}\Phi_{(j+n)}(x)$,

Theorem A2. *If* $\phi(x,t) = x^m t^n$, *then,*

$$\Phi_j(x) = x^m\delta(j-n) = \begin{cases} 1 & \text{if } j = n, \\ 0 & \text{otherwise.} \end{cases}$$

Theorem A3. *If* $\phi(x,t) = \phi(x,t)\frac{\partial^n}{\partial t^n}\phi(x,t)$, *then* $\Phi_j(x) = \sum_{r=0}^{j}\Phi_r(x)\frac{\partial}{\partial x}\Phi_{r-j}(x)$.

Similarly the initial condition takes the form

$$\Phi_0(x) = \phi_0, \tag{A12}$$

where $\Phi_j(x)$ in Equation (A11) is the transform function of the original function $\phi(x,t)$. For $j = 0, 1, 2$ a few terms are

$$\Phi_1(X) = -R(\Phi_0(x)) - N(\Phi_0(x)), \quad \Phi_2(x) = -R(\Phi_1(x)) - N(\Phi_1(x)),$$
$$\Phi_3(x) = -R(\Phi_2(x)) - N(\Phi_2(x)).$$

With the help of Equation (A12) and using the inverse differential transform (A8), we obtain the following approximate solution:

$$\phi(x,t) = \sum_{j=0}^{n} \Phi_j(x) t^j. \tag{A13}$$

References

1. Irfan, M.; Alam, I.; Ali, A.; Shah, K.; Abdeljawad, T. Electron-acoustic solitons in dense electron–positron–ion plasma: Degenerate relativistic enthalpy function. *Results Phys.* **2022**, *38*, 105625. [CrossRef]
2. Demiray, H. Modulation of Electron-Acoustic Waves in a Plasma with Vortex Electron Distribution. *Int. J. Nonlinear Sci. Numer. Simul.* **2015**, *16*, 61–66. [CrossRef]
3. Guo, R. The electron acoustic waves in plasmas with two kappa-distributed electrons at the same temperatures and immobile ions. *Phys. Plasmas* **2021**, *28*, 082105. [CrossRef]
4. Bukhari, S.; Hussain, S.; Irfan, M.; Ali, S. Streaming instability of electron-acoustic waves with nonextensive q-distributed electrons. *Chin. J. Phys.* **2022**, *80*, 253–260. [CrossRef]
5. Dubouloz, N.; Pottelette, R.; Malingre, M.; Treumann, R.A. Generation of broadband electrostatic noise by electron acoustic solitons. *Geophys. Res. Lett.* **1991**, *18*, 155–158. [CrossRef]
6. Montgomery, D.S.; Focia, R.J.; Rose, H.A.; Russell, D.A.; Cobble, J.A.; Fernandez, J.C.; Johnson, R.P. Observation of stimulated electronacoustic-wave scattering. *Phys. Rev. Lett.* **2001**, *87*, 155001. [CrossRef] [PubMed]
7. Singh, S.; Lakhina, G. Generation of electron-acoustic waves in the magnetosphere. *Planet. Space Sci.* **2001**, *49*, 107–114. [CrossRef]
8. Pottelette, R.; Ergun, R.E.; Treumann, R.A.; Berthomier, M.; Carlson, C.W.; McFadden, J.P.; Roth, I. Modulated electron-acoustic waves in auroral density cavities: FAST observations. *Geophys. Res. Lett.* **1999**, *26*, 2629–2632. [CrossRef]
9. Tokar, R.L.; Gary, S.P. Electrostatis hiss and the beam driven electron acoustic instability in the dayside polar cusp. *Geophys. Res. Lett.* **1984**, *11*, 1180–1183. [CrossRef]
10. Mace, R.L.; Hellberg, M.A. Higher-order electron modes in a twoelectron-temperature plasma. *J. Plasma Phys.* **1990**, *43*, 239–255. [CrossRef]
11. Mamun, A.A.; Shukla, P.K.; Eliasson, B. Arbitrary amplitude dust ion-acoustic shock waves in a dusty plasma with positive and negative ions. *Phys. Plasmas* **2009**, *16*, 114503. [CrossRef]
12. Mace, R.L.; Baboolal, S.; Bharuthram, R.; Hellberg, M.A. Arbitrary-amplitude electron-acoustic solitons in a two-electron-component plasma. *J. Plasma Phys.* **1991**, *45*, 323–338. [CrossRef]
13. Berthomier, M.; Pottelette, R.; Malingre, M.; Khotyainsev, Y. Electronacoustic solitons in an electron-beam plasma system. *Phys. Plasmas* **2000**, *7*, 2987–2994. [CrossRef]
14. Xue, J.K. A spherical KP equation for dust acoustic waves. *Phys. Lett. A* **2003**, *314*, 479–483. [CrossRef]
15. Sahu, B.; Roychoudhury, R. Exact solutions of cylindrical and spherical dust ion acoustic waves. *Phys. Plasmas* **2003**, *10*, 4162–4165. [CrossRef]
16. Leblond, H. The reductive perturbation method and some of its applications. *J. Phys. At. Mol. Opt. Phys.* **2008**, *41*, 043001. [CrossRef]
17. Khalid, K.; Ali, A.; Irfan, M.; Algahtani, O. Time-fractional electron-acoustic shocks in magnetoplasma with superthermal electrons. *Alex. Eng. J.* **2022**, *65*, 531–542.
18. Khalid, K.; Algahtani, O.; Irfan, M.; Ali, A. Electron-acoustic solitary potential in nonextensive streaming plasma. *Sci. Rep.* **2022**, *12*, 15175.
19. Killen, M.S.; Johnson, R.S. Propagation of axi-symmetric nonlinear shallow water waves over slowly varying depth. *Math. Comput. Simul.* **2001**, *55*, 463–472. [CrossRef]
20. Radin, D.; Frisch, M.; Valente, G. Symmetries and asymmetries in physics. *Synthese* **2021**, *199*, 983–989.
21. Jehan, N.; Mahmood, S.; Mirza, A.M. Cylindrical and spherical ion-acoustic solitons in adiabatically hot electron–positron–ion plasmas. *Phys. Scr.* **2007**, *76*, 661–664. [CrossRef]
22. Mamun, A.A.; Shukla, P.K. Electron-acoustic solitary waves via vortex electron distribution. *J. Geophys. Res. Atmos.* **2002**, *107*, SIA 15-1–SIA 15-5. [CrossRef]

23. El-Labany, S.K.; El-Taibany, W.F.; Zedan, N.A. Modulated ion acoustic waves in a plasma with Cairns-Gurevich distribution. *Phys. Plasmas* **2017**, *24*, 112118. [CrossRef]
24. Zhou, J.K. *Differential Transformation and Its Applications for Electrical Circuits*; Huazhong University Press: Wuhan, China, 1986.
25. Keskin, Y.; Oturanc, G. Reduced differential transform method for partial differential equations. *Int. J. Nonlinear Sci. Numer. Simul.* **2009**, *10*, 741–749. [CrossRef]
26. Keskin, Y.; Oturanc, G. The reduced differential transform method: A new approach to fractional partial differential equations. *Nonlinear Sci. Lett. A* **2010**, *1*, 207–217.
27. Keskin, Y.; Oturanç, G. Reduced Differential Transform Method for Generalized KdV Equations. *Math. Comput. Appl.* **2010**, *15*, 382–393. [CrossRef]
28. Abdou, M.A. Fractional reduced differential transform method and its applications. *J. Nonlinear Sci. Numer. Simul.* **2018**, *26*, 55–64.
29. Al-Amr, M.O. New applications of reduced differential transform method. *Alex. Eng. J.* **2014**, *53*, 243–247. [CrossRef]
30. Abazari, R. Numerical simulation of coupled nonlinear Schro¨dinger equation by RDTM and comparison with DTM. *J. Appl. Sci.* **2011**, *11*, 3454–3463. [CrossRef]
31. Acan, O.; Firat, O.; Keskin, Y. Conformable variational iteration method, conformable fractional reduced differential transform method and conformable homotopy analysis method for non-linear fractional partial differential equations. *Waves Random Complex Media* **2018**, *30*, 250–268. [CrossRef]
32. Ghosh, S.K.; Gupta, S.K.; Chatterjee, P. Exact solution of the cylindrical Korteweg—de Vries equation for dust ion acoustic wave in unmagnetised plasma. *Phys. Scr.* **2015**, *90*, 125601. [CrossRef]
33. Nakamura, A. The Miura transform and the existence of an infinite number of conservation laws of the cylindrical KdV equation. *Phys. Lett. A* **1981**, *82*, 111–112. [CrossRef]
34. Anishchenko, V.S.; Vladimir, A.; Alexander, N.; Tatjana, V.; Schimansky-Geier, L. *Nonlinear Dynamics of Chaotic and Stochastic Systems: Tutorial and Modern Developments*; Springer: Berlin/Heidelberg, Germany, 2007.
35. Saha, A.; Tamang, J. Effect of q-nonextensive hot electrons on bifurcations of nonlinear and supernonlinear ion-acoustic periodic waves. *Adv. Space Res.* **2018**, *63*, 1596–1606. [CrossRef]